Regular Article

blood

Check for updates

MYELOID NEOPLASIA

JAK2 exon 12 mutant mice display isolated erythrocytosis and changes in iron metabolism favoring increased erythropoiesis

Jean Grisouard,[1,*] Sai Li,[1,*] Lucia Kubovcakova,[1] Tata Nageswara Rao,[1] Sara C. Meyer,[1] Pontus Lundberg,[1] Hui Hao-Shen,[1] Vincent Romanet,[2] Masato Murakami,[2] Thomas Radimerski,[2] Stephan Dirnhofer,[3] and Radek C. Skoda[1]

[1]Department of Biomedicine, Experimental Hematology, University Hospital Basel, Basel, Switzerland; [2]Disease Area Oncology, Novartis Institutes for Biomedical Research, Basel, Switzerland; and [3]Institute of Pathology, University Hospital Basel, Basel, Switzerland

Key Points

- Mice expressing a *JAK2 exon 12* mutation display isolated erythrocytosis similar to the majority of patients with *JAK2 exon 12* mutations.
- *JAK2 exon 12* mutation induces changes in iron metabolism that increase iron availability to allow maximal production of red cells.

Mutations in *JAK2 exon 12* are frequently found in patients with polycythemia vera (PV) that do not carry a *JAK2-V617F* mutation. The majority of these patients display isolated erythrocytosis. We generated a mouse model that expresses *JAK2-N542-E543del,* the most frequent *JAK2 exon 12* mutation found in PV patients. Mice expressing the human *JAK2-N542-E543del (Ex12)* showed a strong increase in red blood cell parameters but normal neutrophil and platelet counts, and reduced overall survival. Erythropoiesis was increased in the bone marrow and spleen, with normal megakaryopoiesis and absence of myelofibrosis in histopathology. Erythroid progenitors and precursors were increased in hematopoietic tissues, but the numbers of megakaryocytic precursors were unchanged. Phosphorylation Stat3 and Erk1/2 proteins were increased, and a trend toward increased phospho-Stat5 and phospho-Stat1 was noted. However, Stat1 knock out in *Ex12* mice induced no changes in platelet or red cell parameters, indicating that Stat1 does not play a central role in mediating the effects of Ex12 signaling on megakaryopoiesis or erythropoiesis. *Ex12* mice showed decreased expression of *hepcidin* and increased expression of *transferrin receptor-1* and *erythroferrone,* suggesting that the strong erythroid phenotype in *Ex12* mutant mice is favored by changes in iron metabolism that optimize iron availability to allow maximal production of red cells. (*Blood.* 2016;128(6):839-851)

Introduction

The *JAK2-V617F* mutation occurs in the vast majority (>95%) of patients with polycythemia vera (PV).[1-4] PV patients who are negative for *JAK2-V617F* frequently carry a mutation in *exon 12* of *JAK2*.[5] These *JAK2 exon 12* mutations alter various nucleotide positions in the vicinity of codon 539 and often involve deletions of 1 to 3 codons.[5-8] In a large collaborative study on 106 cases, patients with *JAK2 exon 12* mutations have been found to have significantly higher hemoglobin values and lower platelet and leukocyte counts at diagnosis, but similar survival and incidences of thrombosis, myelofibrosis, and leukemia as patients with *JAK2*-V617F.[9] Two-thirds of patients with *JAK2 exon 12* mutation cases manifested as pure erythrocytosis, whereas the remaining patients had erythrocytosis plus leukocytosis and/or thrombocytosis. No differences in phenotype have been linked to the presence of a particular mutation subtype.[9] The *JAK2 exon 12* mutations have been included in the World Health Organization diagnostic criteria for PV.[10]

Scott et al showed in a retroviral transplantation model that recipients of mouse bone marrow (BM) cells transduced with *Jak2*-K539L displayed elevated hemoglobin, reticulocytosis, and a pronounced leukocytosis.[5] Furthermore, exon 12 mutations were associated with constitutive, erythropoietin (Epo)-independent activation of Jak2, Stat5, and Erk1/2.[5] Recently, the transcriptional profiles of erythroid colonies from PV patients with *JAK2 exon 12* mutations were examined and a Stat1 signature was found.[11]

To study the biology of PV caused by a *JAK2 exon 12* mutation in more detail, we generated an inducible transgenic mouse model using a bacterial artificial chromosome (BAC) carrying the human *JAK2* gene. For the transgene construct, we selected the *JAK2-N542-E543del* mutation because it is the most frequent subtype, occurring in ~30% of PV patients with a *JAK2 exon 12* mutation.[9] Here we present a detailed phenotypic and molecular characterization of the *JAK2-N542-E543del* mutant mice.

Methods

Transgenic mice

The human *JAK2-N542-E543del* transgene was constructed by modifying a BAC containing the wild-type (WT) human *JAK2* gene.[12] A fragment containing *JAK2*

Submitted December 22, 2015; accepted June 5, 2016. Prepublished online as *Blood* First Edition paper, June 10, 2016; DOI 10.1182/blood-2015-12-689216.

*J.G. and S.L. contributed equally to this study.

The online version of this article contains a data supplement.

There is an Inside *Blood* Commentary on this article in this issue.

The publication costs of this article were defrayed in part by page charge payment. Therefore, and solely to indicate this fact, this article is hereby marked "advertisement" in accordance with 18 USC section 1734.

© 2016 by The American Society of Hematology

Downloaded from http://ashpublications.net/blood/article-pdf/128/6/839/1398408/839.pdf by guest on 18 May 2024

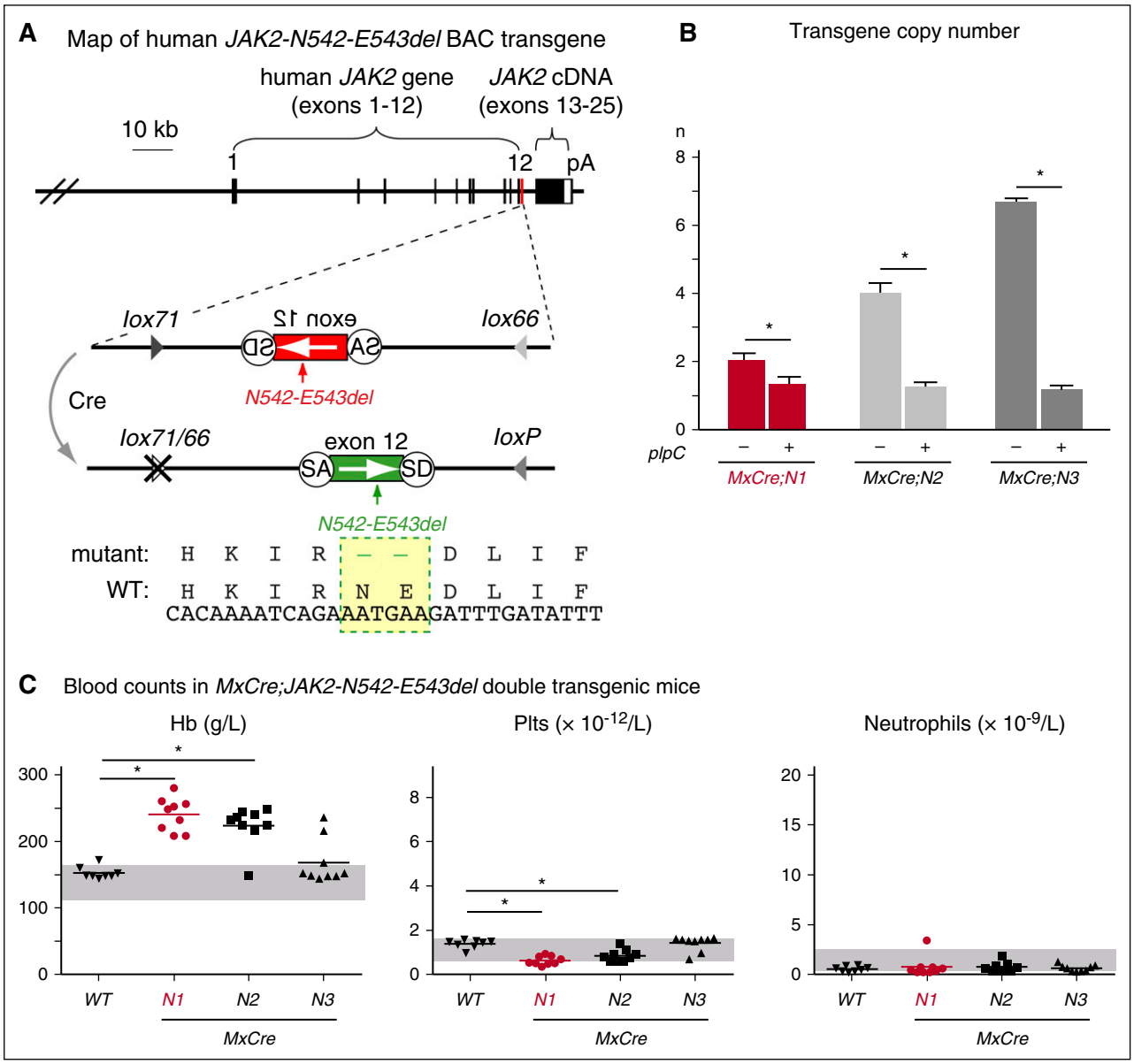

Figure 1. Generation and characterization of *JAK2-Ex12* transgenic lines. (A) Map of the human *JAK2* BAC carrying the *N542-E543del* mutation in exon 12 (shown in red). The mutated region is shown enlarged below. In the presence of Cre recombinase, the mutated *exon 12* is flipped from the inverse orientation (red) to the correct orientation (green). Recombination generates 1 WT *loxP* and 1 double-mutant *lox66/77* site, which is no longer substrate for Cre recombinase. The DNA and amino acid sequences of the mutant (*N542-E543del)* and WT *JAK2* are shown at the bottom. (B) Transgene copy number in 3 transgenic lines, named *N1*, *N2*, and *N3*. These mice were crossed with the IFN-inducible *MxCre* strain and analyzed for transgene copy number (n) by RT-PCR before and 24 weeks after induction with *plpC*. The average values obtained from 3 mice per group are shown with error bars indicating ± SEM. (C) Peripheral blood parameters in *MxCre;N1*, *MxCre;N2*, and *MxCre;N3* double transgenic mice. Blood counts were determined 16 weeks after 1× *plpC* injection. Horizontal lines represent the average values. The group sizes were: n = 9 per double transgenic strain and n = 8 for the WT controls. One-way ANOVA with subsequent Bonferroni post-test was used. **P* < .05. cDNA, complementary DNA; IFN, interferon; Hb, hemoglobin; pA, polyadenylation signal from *SV40*; Plt, platelet; SA, splice acceptor; SD, splice donor.

exon 12 N542-E543del was cloned from a PV patient harboring this mutation and the construct was sequenced. The primers used for *N542-E543del* cloning were: forward 5′-TGCTAACATCTAACACAAGGTTGG-3, and reverse 5′-CAAAGTTCAATGAGTTGACCCC-3′. The human *JAK2-N542-E543del* was introduced into the BAC by homologous recombination in the bacterial strain SW102. To make the transgene construct Cre-inducible, the mutant *JAK2 exon 12* was placed with inverse orientation and flanked by anti-parallel *lox71* and *lox66* (Figure 1A; see also supplemental Figure 1 and supplemental Methods, available on the *Blood* Web site). The purified human *JAK2* DNA was microinjected into pronuclei of oocytes from C57BL/6 mice and transplanted into foster mother recipients. Transgene-positive founder mice were crossed with *MxCre* transgenic mice to get double transgenic mice.[13] Cre expression in *MxCre* mice was induced by a single intraperitoneal injection of 300 μg polyinosine-polycytosine (*pIpC*). Alternatively, *JAK2-N542-E543del* transgene-positive mice were crossed with *SclCre*^{ER} transgenic mice. Cre activity in *SclCre*^{ER} mice was induced by daily injections of 2 mg tamoxifen dissolved in 200 μL sunflower oil for 5 consecutive days.[14] All mice used in this study were kept under specific pathogen-free conditions and in accordance with Swiss federal regulations. To generate triple transgenic mice, *SclCre*^{ER}*;JAK2-N542-E543del* animals were crossed with *Stat1* knockout mice.[15]

Transplantation

Donor mice were euthanized at 24 weeks after *pIpC* injection (5 weeks after tamoxifen induction in *SclCre*^{ER}*;Ex12* mice, respectively) and total BM cells were transplanted into lethally irradiated (12 Gy) C57BL/6 female recipient mice as described previously.[12]

Downloaded from http://ashpublications.net/blood/article-pdf/128/6/839/1398408/839.pdf by guest on 18 May 2024

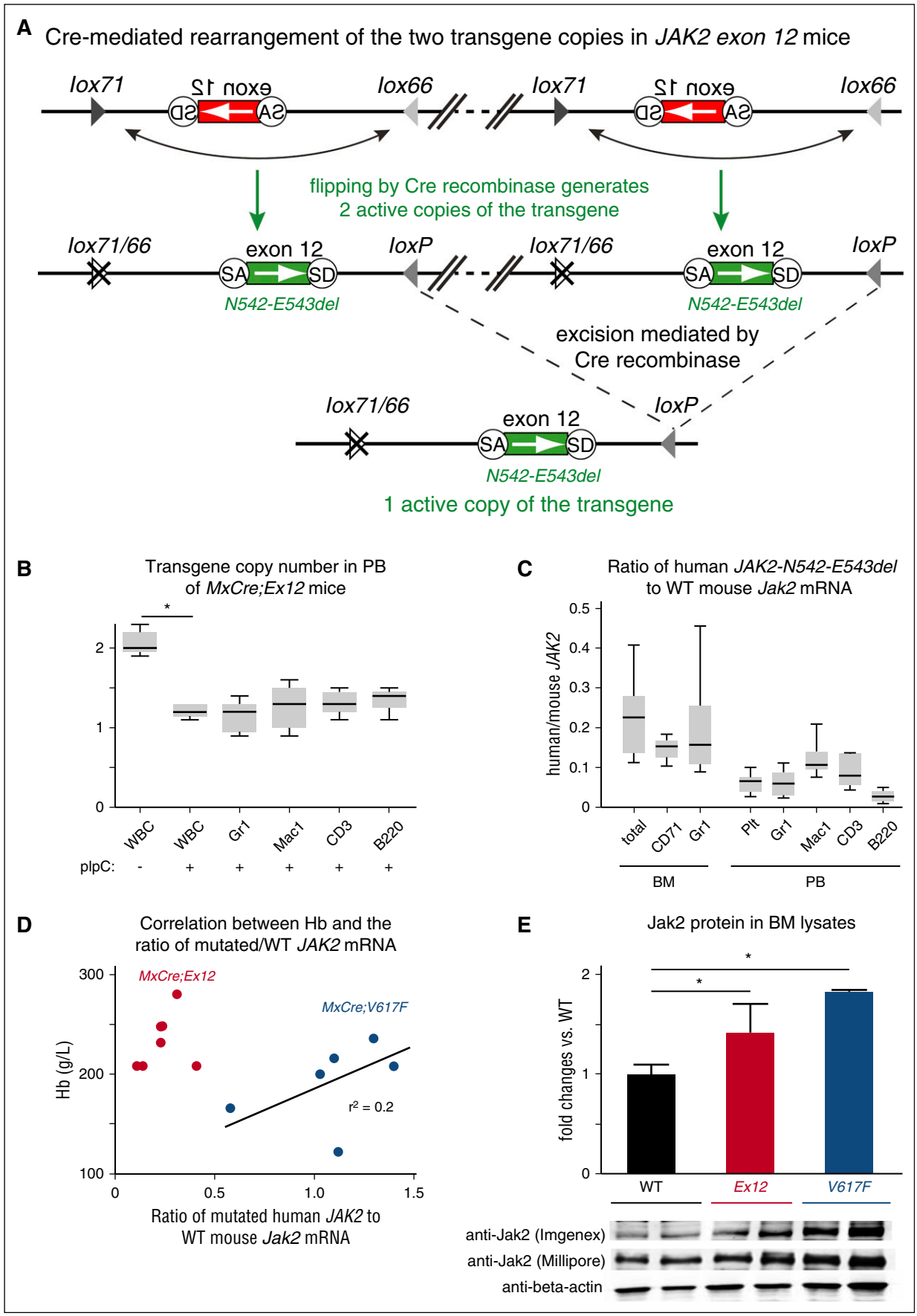

Figure 2.

Downloaded from http://ashpublications.net/blood/article-pdf/128/6/839/1398408/839.pdf by guest on 18 May 2024

Blood and tissue analysis

Blood counts were determined on an Advia 120 Hematology Analyzer using the Multispecies Software (Bayer, Leverkusen, Germany). For histopathological analysis, tissue specimens were fixed in 4% phosphate-buffered formalin and embedded in paraffin. Paraffin sections (4 μm) were stained with hematoxylin and eosin or Gömöri (analysis of the amount and distribution of reticulin fibers).

Hematopoietic progenitor assays

Erythroid burst-forming unit (BFU-E) colonies were scored after 9 to 10 days of culture of BM cells (2×10^5) in methylcellulose-based medium (Stem Alpha, St. Genis L'Argentière, France) supplemented with 100 ng/mL stem cell factor (PeproTech), 310 μg/mL human transferrin and 200 μM hemin (Sigma-Aldrich), and 3 units/mL Epo. Epo-independent erythroid colonies (EECs) were scored after 4 to 5 days of culture in the same media but without Epo. Myeloid progenitor assays were performed with 1×10^4 BM cells in triplicates in M3534 medium (StemCell Technologies, Vancouver, BC, Canada) and colony-forming unit granulocyte (CFU-G), colony-forming unit macrophage (CFU-M), and colony-forming unit granulocyte macrophage (CFU-GM) colonies were counted after 14 days of culture. BM cells (5×10^4) were cultured for 8 days on slide chambers in duplicates with or without 50 ng/mL recombinant human thrombopoietin (Tpo) in supplemented MegaCult-C medium (StemCell Technologies), and colony-forming units–megakaryocyte (CFU-MK) were fixed, stained, and counted.[14]

Real-time polymerase chain reaction (RT-PCR), flow cytometry, phospho-protein analysis, immunohistochemistry, western blot analysis, and meso scale discovery (MSD) assays

See supplemental Methods.

Hepcidin protein assay

Serum from mice was analyzed using the mouse hepcidin competition enzyme-linked immunosorbent assay (ELISA) kit and serum from patients collected at diagnosis was analyzed using the human hepcidin ELISA kit following the manufacturer's instructions (LifeSpan Biosciences, Seattle, WA).

Patient cohort

The collection of blood samples and clinical data were performed at the study center in Basel, Switzerland, and approved by the local Ethics Committees (Ethik Kommission Beider Basel). Written informed consent was obtained from all patients in accordance with the Declaration of Helsinki. The diagnosis of myeloproliferative neoplasm (MPN) was established according to the revised criteria of the World Health Organization.[10]

Statistical analysis

Results are presented as mean ± standard error of the mean (SEM). To assess statistical significance among groups, one-way or two-way analysis of variance (ANOVA) with subsequent Bonferroni post-test (GraphPad Prism, version 6.01) were used, and P values $< .05$ were considered significant.

Results

To generate transgenic mice that carry the human *JAK2* gene with a gain-of-function mutation in *exon 12*, we modified a BAC DNA construct for the WT *JAK2*,[12] and introduced a *N542-E543del* mutation using homologous recombination in bacteria (Figure 1; supplemental Figure 1). The mutated *exon 12* was placed in the reverse orientation flanked by antiparallel *loxP* sites. In this configuration, no full length Jak2 protein can be made, because the messenger RNA (mRNA) is truncated after *exon 11*. Expression of Cre recombinase results in flipping the orientation of the *exon 12*, thereby restoring a functionally active transgene (Figure 1A). To make the recombination unidirectional and irreversible, we used modified versions of the *loxP* site named *lox66* and *lox71*.[16] Recombination between antiparallel *lox66* and *lox71* sites create 1 WT *loxP* site and 1 double-mutant site (*lox66/71*) with greatly reduced affinity for Cre. Using this BAC construct, we generated 3 transgenic lines in the inbred C57BL/6 background, named *N1*, *N2*, and *N3* that differed in transgene copy numbers (Figure 1B). Offspring of these 3 lines was crossed with the IFN-inducible *MxCre* strain.[13] Upon injection of *pIpC* and activation of the transgene by Cre recombinase, 2 transgenic lines displayed a PV phenotype with elevated hemoglobin values and platelets slightly lower than WT controls, whereas in the third line (*N3*) only a subset of mice developed PV (Figure 1C). The transgenic line *N1* was selected for detailed analysis.

We found that the *N1* line strain (hereafter called *Ex12*) carries 2 copies of the transgene that integrated in a "head-to-tail" configuration (Figure 2A). Due to the orientation of the 4 *loxP* sites, Cre recombinase can activate and/or excise copies of the transgene, yielding 1 or 2 copies of the transgene in the active orientation. After induction of the transgene in *MxCre;Ex12* mice by *pIpC,* the transgene copy number decreased from 2 to 1 in all subsets of peripheral blood cell types (Figure 2B). Expression of the transgenic *JAK2-Ex12* mRNA was determined by quantitative PCR and plotted as the ratio between the mutant human *JAK2-Ex12* and the WT mouse *Jak2* (Figure 2C). Total BM, as well as erythroid and myeloid subsets of BM cells expressed the mutant *JAK2* at about 20% of the WT, whereas the expression of the mutant *JAK2* in peripheral blood cells was lower (around 10%). Expression was lowest in B cells. We previously showed that the ratio of mutant *JAK2-V617F* to WT *Jak2* in BM cells in *MxCre;FF1* mice (hereafter called *MxCre;V617F*) correlated with the hemoglobin levels.[12] Here, we confirmed this correlation (Figure 2D, blue dots). The expression ratio of the mutant *JAK2-Ex12* was substantially lower than that of *JAK2-V617F*, but despite the lower expression the hemoglobin levels were higher (Figure 2D, red dots). Jak2 protein

Figure 2. Analysis of *JAK2-Ex12* transgene copy number and transgene expression. (A) Schematic drawing of Cre-mediated rearrangements of the *JAK2-Ex12* transgene. The region of the transgene containing the mutated *JAK2 exon 12* is shown enlarged and the DNA connecting the 2 copies of the transgene was omitted (inclined double lines connected by dashed line). The head-to-tail orientation of the 2 copies of the transgene was confirmed by PCR with primers flanking the ends of the construct. The inactive transgene configuration (top); Cre recombination of adjacent *loxP* sites (middle) leads to reversal of the orientation and activation of 2 copies of the transgene (*N542-E543del)*; and Cre recombination of distant *loxP* sites that are in parallel orientation results in the excision of 1 copy of the transgene (bottom). (B) The *Ex12* transgene copy number was determined by quantitative PCR in white blood cells (WBCs), and in sorted $Gr1^+$, $Mac1^+$, $CD3^+$, and $B220^+$ cells from peripheral blood (PB) of *MxCre;Ex12* mice 24 weeks after *pIpC* injection (n = 6 mice per group). (C) Ratio of human *JAK2-N542-E543del* to mouse *Jak2* mRNA expression determined by RT-PCR in BM and peripheral blood. Results from total BM cells or sorted erythroid ($CD71^+$) and myeloid ($Gr1^+$) cells, as well as platelets, granulocytes ($Gr1^+$), monocytes ($Mac1^+$), T cells ($CD3^+$), and B cells ($B220^+$) from peripheral blood of *MxCre;Ex12* mice 24 weeks after *pIpC* induction are shown. Boxes represent the interquartile range that contains 50% of the values and the whiskers indicating the range containing 95% of the values. Horizontal lines indicate the mean values (n = 6 mice per group). (D) Correlation of hemoglobin levels with the ratio between human mutated *JAK2*/mouse wild-type (WT) *Jak2* mRNA expression in BM of *MxCre;Ex12* (red dots, n = 7) and *MxCre;V617F* mice (blue dots, n = 6), 24 weeks after *pIpC* induction. (E) Immunoblot analysis of Jak2 protein expression in BM cell lysates. The upper panel shows the quantification of western blots probed with an antibody that preferentially recognizes human Jak2 protein (Imgenex). The intensities of the bands in the lower panel were quantified and differences in loading were normalized using β-actin antibodies. The values are shown as the fold change of Jak2 in WT mice. For comparison, the blot was reprobed with a Jak2 antibody (Millipore) that does not discriminate between human and mouse Jak2 proteins. WT (black), *MxCre;Ex12* (red), and *MxCre;V617F* (blue) mice (n = 2 per group). One-way ANOVA with subsequent Bonferroni post-test was used. $*P < .05$.

Downloaded from http://ashpublications.net/blood/article-pdf/128/6/839/1398408/839.pdf by guest on 18 May 2024

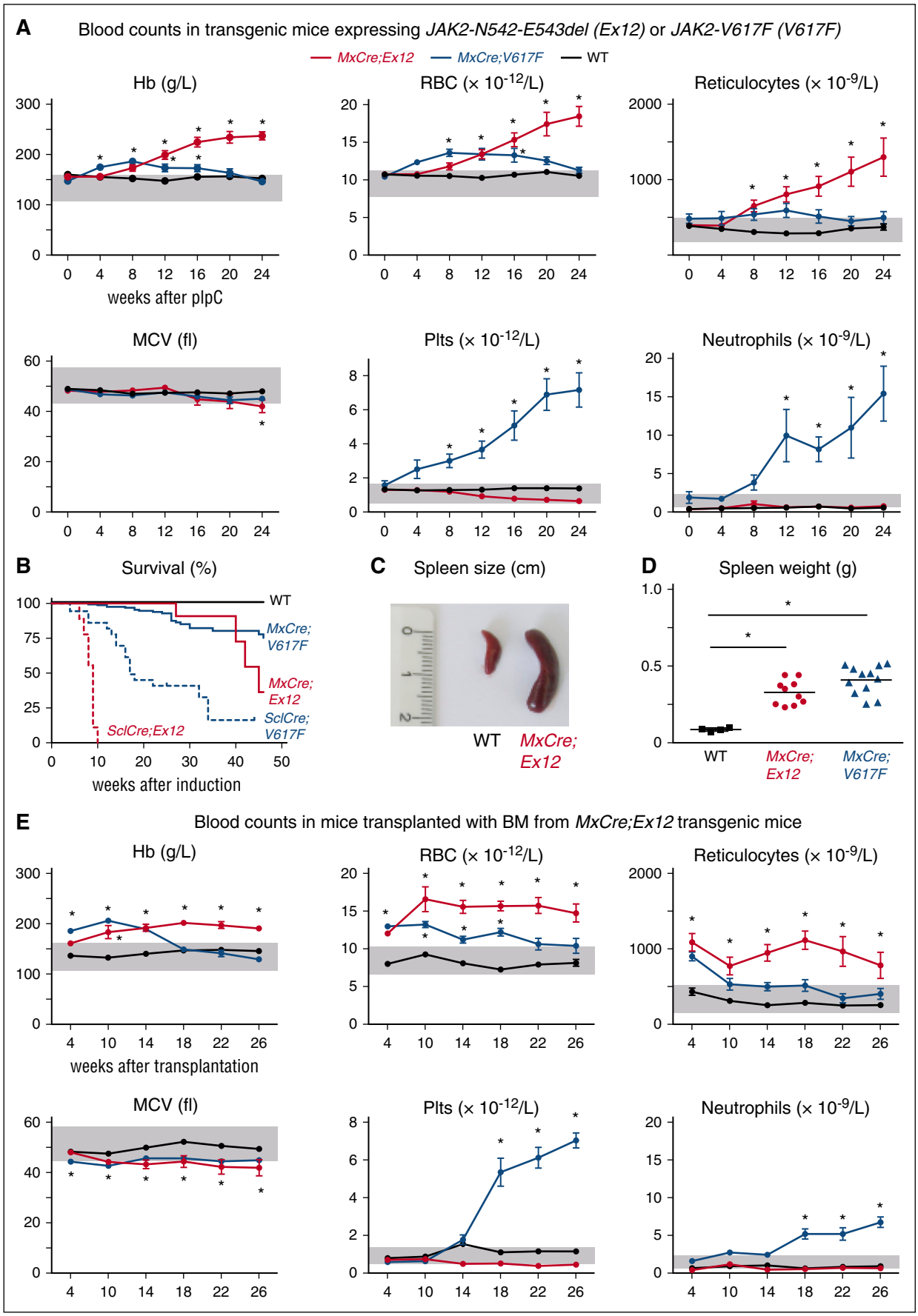

Figure 3.

Downloaded from http://ashpublications.net/blood/article-pdf/128/6/839/1398408/839.pdf by guest on 18 May 2024

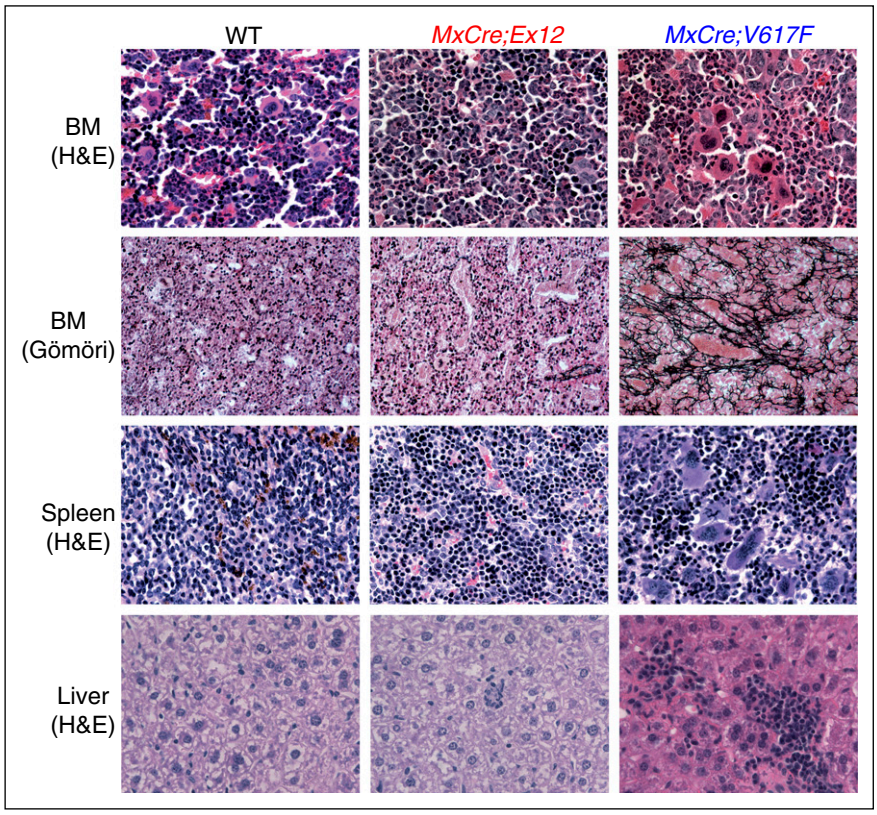

Figure 4. Histopathology of transgenic mice and controls. Mice were euthanized 24 weeks after *plpC* injection. H&E staining of BM, spleen, and liver, as well as reticulin-staining (Gömöri) of BM are shown (original magnification ×400). H&E, hematoxylin and eosin.

expression was assessed in BM cells by immunoblot analysis using 2 different anti-Jak2 antibodies (Figure 2E). A slight increase in total Jak2 protein was noted in both *MxCre;Ex12* and *MxCre;V617F* mice compared with WT. This difference was more pronounced using an antibody (Imgenex) that preferentially detects the human Jak2 over mouse Jak2. A trend toward increased Jak2 protein was observed in *MxCre;V617F* mice compared with *MxCre;Ex12* mice.

The time course of blood parameters in *MxCre;Ex12* mice after induction with *plpC* is shown in Figure 3A, and compared with our previously described *MxCre;V617F* mice and WT controls. *MxCre;Ex12* mice displayed a pure erythrocytosis phenotype with hemoglobin values higher than in the *MxCre;V617F* mice. In contrast, the platelet values in *MxCre;Ex12* mice were normal or at later stages slightly lower than in WT controls (Figure 3A, lower panel). Similarly, neutrophils also remained normal. The same phenotype but with faster kinetics was observed in $SclCre^{ER}$*;Ex12* mice after induction with tamoxifen (supplemental Figure 2A). $SclCre^{ER}$*;Ex12* mice showed a dramatically shortened survival with all mice dying within 10 weeks after induction (Figure 3B). Some $SclCre^{ER}$*;Ex12* mice that died prematurely showed intraperitoneal bleeding (data not shown). Increased spleen size and spleen weight was observed in all mice expressing the *JAK2-Ex12* mutation (Figure 3C-D; supplemental Figure 2B).

The PV phenotype of *MxCre;Ex12* and $SclCre^{ER}$*;Ex12* mice was transplantable into lethally irradiated mice (Figure 3E; supplemental Figure 2C). The onset of MPN in these recipient mice was slightly earlier than in nontransplanted mice, because BM from pre-induced donors that already displayed MPN have been used for the transplantations. The red cell parameters in recipients transplanted with *MxCre;Ex12* BM were comparable with the nontransplanted *MxCre;Ex12* mice, with slightly lower MCV and reticulocyte counts (Figure 3E). In recipients transplanted with $SclCre^{ER}$*;Ex12* BM, the MCV was clearly lower and the hemoglobin values declined after 18 to 24 weeks (supplemental Figure 2C). Hemoccult tests of stool in these mice showed evidence of gastrointestinal bleeding (supplemental Figure 3A) and spleen weight was elevated (supplemental Figure 3B). Recipients transplanted with BM from *Ex12* or *V617F* strains showed longer survival that the corresponding nontransplanted mice, suggesting that expression of mutant *JAK2* in nonhematopoietic tissues contributes to lethality. In the transplantation setting, mouse mutants activated by $SclCre^{ER}$ showed shorter survival than mutants activated by *MxCre* (supplemental Figure 3C), as also observed in the nontransplanted mutants (Figure 3B). The PV phenotype was also transplantable into secondary recipients (data not shown).

Histopathological analysis of *MxCre;Ex12* mice revealed hypercellular BM and erythroid hyperplasia but only a slight increase of MKs (Figure 4). Clustering of MKs as present in *MxCre;V617F* mice was not observed in *MxCre;Ex12* mice. The histologic architecture of the spleen was partly replaced with increased erythropoiesis and islands of hematopoiesis were also detectable in the liver. In contrast to the *MxCre;V617F* mice, the

Figure 3. Phenotypes of mice expressing the *JAK2-Ex12* transgene. *MxCre;Ex12* double transgenic mice were compared with *MxCre;V617F* mice (ie, mice expressing the *JAK2-V617F* transgene) and WT control mice. (A) Time course of blood counts (average ± SEM) before *plpC* injection (0) and every 4 weeks after *plpC* injection is shown. The group sizes were: *MxCre;Ex12* (n = 15), *MxCre;V617F* (n = 10), and WT (n = 13). (B) Survival of mice is shown. (C) Picture of a spleen from a *MxCre;Ex12* and a WT mouse 24 weeks after *plpC*. (D) Spleen weight of *MxCre;Ex12* (n = 10), *MxCre;V617F* (n = 12), and WT mice (n = 4) 24 weeks after *plpC*. (E) Time course of blood counts in C57BL/6 lethally irradiated recipient mice transplanted with BM cells from *MxCre;Ex12*, *MxCre;V617F*, or WT donor mice (n = 8 mice per group). One-way ANOVA with subsequent Bonferroni post-test was used. *$P < .05$. MCV, mean corpuscular volume; RBC, red blood cell.

Downloaded from http://ashpublications.net/blood/article-pdf/128/6/839/1398408/839.pdf by guest on 18 May 2024

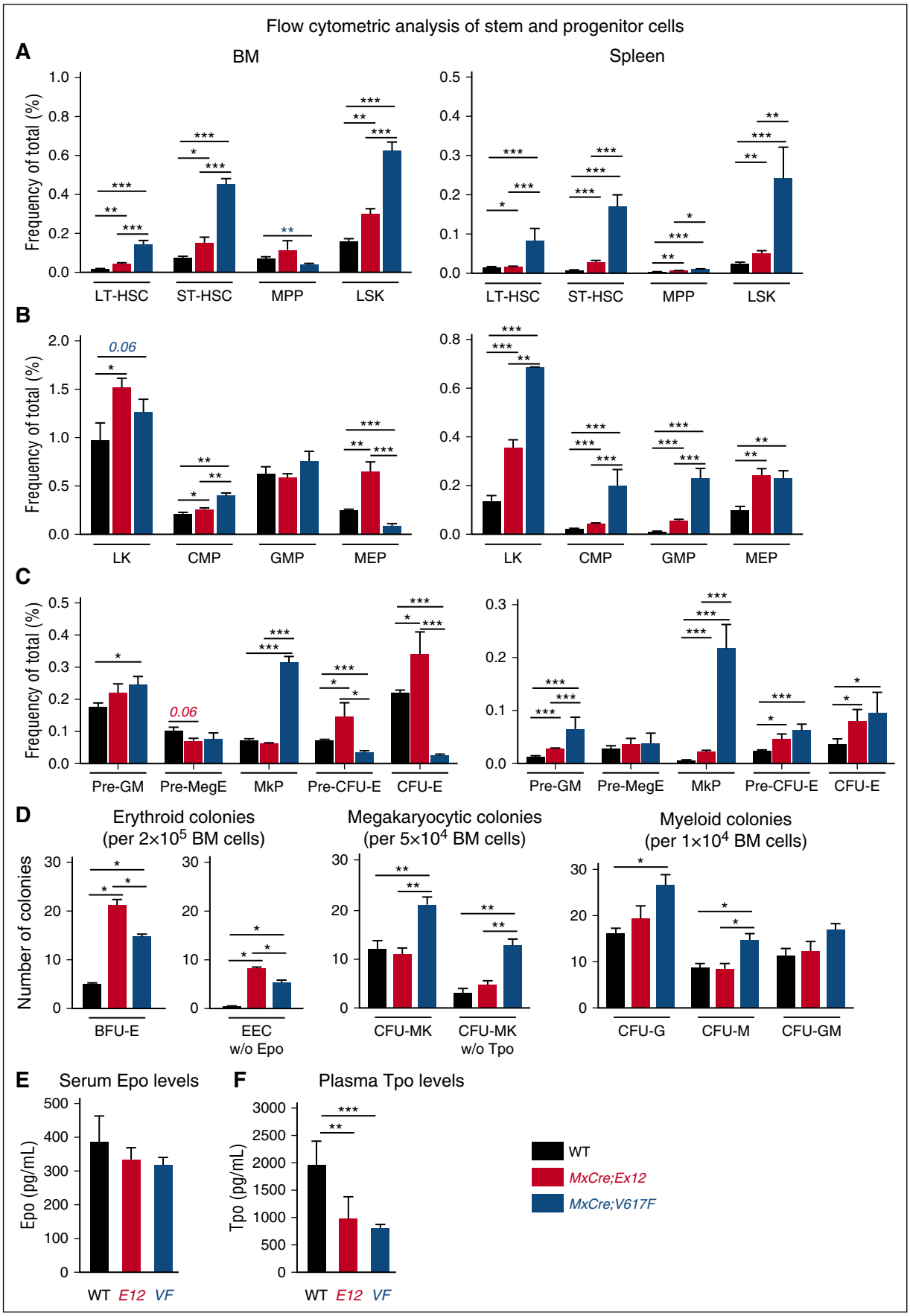

Figure 5.

Downloaded from http://ashpublications.net/blood/article-pdf/128/6/839/1398408/839.pdf by guest on 18 May 2024

MxCre;Ex12 mice displayed no increase in reticulin fibers or other signs of myelofibrosis (Figure 4).

To assess the hematopoietic progenitor and stem cell compartment of *Ex12* mice in more detail, we performed flow cytometry analysis and progenitor colony assays (Figure 5). Compared with WT controls, *MxCre;Ex12* and *MxCre;V617F* mice displayed increased frequencies of early HSC and progenitor cell populations in the BM and spleen (Figure 5A). The proportion of $Sca1^-/c\text{-}Kit^+$ cells in Lin^- population cells was increased in both *JAK2* mutant strains (Figure 5B). Accordingly, the frequency of common myeloid progenitors and granulocyte-monocyte progenitors was also significantly increased in *MxCre;Ex12* mice (Figure 5B). Analysis of MK-erythrocyte progenitors and erythroid committed precursors (ie, CFU-E) revealed a pronounced increase in BM of *MxCre;Ex12* mice as compared with WT controls, but were reduced in the BM of *MxCre;V617F* mice, consistent with earlier results.[17] In the spleen, the proportion of CFU-E cells was increased overall and was even higher in *Ex12* than in *V617F* mice (Figure 5C). In contrast, cells of the megakaryocytic progenitors were unchanged in *MxCre;Ex12* mice in comparison with WT controls, but were increased in the BM and spleen of *MxCre;V617F* mice (Figure 5C).

Colony assays in semisolid media revealed that BFU-E colonies were increased, and growth of EECs occurred in *Ex12* and *V617F* mice (Figure 5D). Interestingly, both BFU-E and EEC numbers were enhanced in *MxCre;Ex12* mice compared with *MxCre;V617F* mice. The numbers of CFU-MK were not increased in *MxCre;Ex12* mice compared with WT controls, whereas *MxCre;V617F* mice showed increased CFU-MK in presence and absence of Tpo. No significant differences in myeloid colonies were detected between *MxCre;Ex12* mice and WT controls, whereas granulocyte CFU and macrophage CFU were increased in *MxCre;V617F* mice. Overall, erythroid progenitors and precursors were elevated in *Ex12* mice, but megakaryopoiesis was not significantly altered compared with WT. As expected, serum Epo levels were slightly reduced in *Ex12* and *V617F* mice compared with WT controls (Figure 5E). Despite normal platelet counts, *Ex12* mice showed decreased Tpo plasma levels (Figure 5F). Plasma Tpo was strongly suppressed in *V617F* mice, which display thrombocytosis and are expected to effectively remove Tpo from circulation.

To assess the differences in signaling, we analyzed the phosphorylation of Stat5, Stat3, and Stat1 proteins, as well as Akt and Erk1/2 that are known downstream targets of the Jak2 kinase. Western blot analysis of BM cell lysates using phospho-protein–specific antibodies revealed significantly increased baseline levels of pStat3 and pErk1/2, and a trend toward increased pStat5 and pStat1 in *Ex12* mice compared with WT controls (Figure 6A). No significant changes in the phosphorylation of Stat5 or Stat3 were detected by immunohistochemistry staining of nuclei, phospho-flow analysis, or MSD analysis when comparing *Ex12* mice with WT controls (Figure 6B-C). Phospho-flow analysis revealed no differences in phosphorylation of Stat1 and Erk1/2 in BM and spleen of *Ex12* mice, and WT controls (Figure 6D-E), but decreased pAkt was noted in spleen cells of E12 and V617F mice (Figure 6F).

Because we observed a trend toward increased pStat1 in western blots of *MxCre;Ex12* BM cells, and this finding is unexpected given the proposed role of Stat1 in promoting megakaryopoiesis in the context of *JAK2*-V617F,[18,19] we sought to clarify the role of Stat1 in Jak2-Ex12 signaling by analyzing *Ex12;Stat1*$^{-/-}$ double-mutant mice (Figure 6G-H).[15] To obtain sufficient numbers of triple transgenic mice for study, we transplanted BM cells from *SclCre;Ex12;Stat1*$^{-/-}$, *SclCre;Ex12;Stat*$^{+/+}$, and controls, and induced expression of *Jak2;Ex12* with tamoxifen. We observed no differences in blood counts or survival in mice expressing *Jak2;Ex12* on *Stat*$^{+/+}$ or *Stat1*$^{-/-}$ backgrounds (Figure 6G). A trend toward slightly lower spleens was noted in *Ex12;Stat1*$^{-/-}$ mice compared with *Ex12;Stat*$^{+/+}$ mice, but this difference was not significant. We also did not observe differences in erythroid, megakaryocytic, or myeloid precursors in the BM or spleens of these mice (Figure 6H).

Because *Ex12* mice display a predominantly erythroid phenotype, we compared mRNA expression of selected genes implicated in erythropoiesis and found that the *transferrin receptor-1* (*Tfr1*) mRNA was increased in *MxCre;Ex12* mice compared with WT, whereas *MCL-1*, *BCL-XL*, and *oncostatin M* showed no significant differences (Figure 7A). These results suggested that iron metabolism could be altered in *Ex12* mice. In addition, the expression of Tfr1 protein (also called CD71) was found to be increased in BM cells of *MxCre;Ex12* mice by flow cytometry, indicating that Tfr1 protein was upregulated at the cell surface on a per cell basis (Figure 7B). Serum iron levels showed no significant differences (Figure 7C), whereas liver iron stores were increased in *MxCre;V617F* mice (Figure 7D). Expression of the key iron regulatory gene *Hepcidin* (*Hamp*) was decreased in the peripheral blood and liver from *MxCre;Ex12* mice (Figure 7E) and a trend toward lower hepcidin protein levels was also observed in serum (Figure 7F). *Erythroferrone* (*Erfe*) (*Fam132b*), an erythroid regulator of iron metabolism and suppressor of *Hamp* was strongly increased in the peripheral blood and spleen of *Ex12* transgenic mice (Figure 7G). These changes were also observed in *SclCre*^{ER}*;Ex12 mice* (supplemental Figure 4). To determine whether similar alterations also occur in patients with PV, we measured hepcidin serum levels and found that they were lowest in patients with *JAK2 exon 12* mutations compared with MPN patients carrying *JAK2-V617F* (Figure 7H). Finally, we analyzed mRNA expression in BFU-E grown in methylcellulose (Figure 7I). BFU-E colonies from patients with *JAK2 exon 12* mutations showed significantly increased *TFR1* mRNA levels compared with colonies from patients with *JAK2-V617F*, but there was no difference between BFU-E colonies positive or negative for the *JAK2 exon 12* mutations (Figure 7I, left panel). In contrast, BFU-E colonies positive for *JAK2 exon 12* mutations expressed more *ERFE* mRNA than colonies genotyped to be WT for *JAK2* (Figure 7I, right panel). These

Figure 5. Analysis of hematopoietic stem and progenitor subsets in *JAK2-Ex12* transgenic mice. (A) Bar graphs shows the average frequency of LT-HSC ($Lin^-Kit^+Sca\text{-}1^+CD150^+CD48^-$), ST-HSC ($Lin^-Kit^+Sca\text{-}1^+CD150^+CD48^+$), MPP ($Lin^-Kit^+Sca\text{-}1^+CD150^{lo}CD48^+$), and LSK in total BM (left) and spleen (right) of indicated mice (n = 5-6 mice per each genotype). (B) Average frequency of myeloid precursors LK, CMP ($Lin^-Kit^+Sca\text{-}1^+$ $CD34^+$ $Fc\gamma RII/III^{lo}$), GMP ($Lin^-Kit^+Sca\text{-}1^+$ $CD34^+$ $Fc\gamma RII/III^+$), and MEP ($Lin^-Kit^+Sca\text{-}1^+$ $CD34^-$ $Fc\gamma RII/III^{lo}$) in total BM (left) and spleen (right) of indicated mice (n = 5-6 mice per each genotype). (C) Average frequency of MK and erythroid committed subsets, Pre-GM ($Lin^-Kit^+Sca\text{-}1^-CD41^{-/+}CD150^-CD105^-$), Pre-MegE ($Lin^-Kit^+Sca\text{-}1^-CD41^{-/+}$ $CD150^+CD105^-$), MkP ($Lin^-Kit^+Sca\text{-}1^-CD41^+$ $CD150^+$), Pre–erythroid CFU (CFU-E) ($Lin^-Kit^+Sca\text{-}1^-CD41^-CD150^+CD105^+$), and CFU-E ($Lin^-Kit^+Sca\text{-}1^-CD41^-CD150^{lo}CD105^+$) in total BM (left) and spleen (right) of indicated mice (n = 5-6 mice per each genotype). Mice were analyzed 16 weeks after *pIpC* injection. (D) Analysis of colonies grown in semisolid media. Numbers on Y-axis indicate the colony counts. (E) Serum Epo levels. (F) Plasma Tpo levels (n = 6 mice per genotype). All data are presented as mean ± SEM. One-way or two-way ANOVA with subsequent Bonferroni post-test was used. $^*P < .05$; $^{**}P < .01$; $^{***}P < .001$. CMP, common myeloid progenitors; GMP, granulocyte-monocyte progenitors; HSC, hematopoietic stem cell; LK, Lin^-cKit^+; LSK, $Lin^-Sca\text{-}1^+cKit^+$; LT-HSC, long-term HSC; MEP, MK-erythrocyte progenitors; MkP, MK progenitors; MPP, multipotent progenitors; Pre-GM, pre–granulocyte-monocyte progenitors; Pre-MegE, Pre–megakaryocyte-erythroid progenitors; ST-HSC, short-term HSC.

Downloaded from http://ashpublications.net/blood/article-pdf/128/6/839/1398408/839.pdf by guest on 18 May 2024

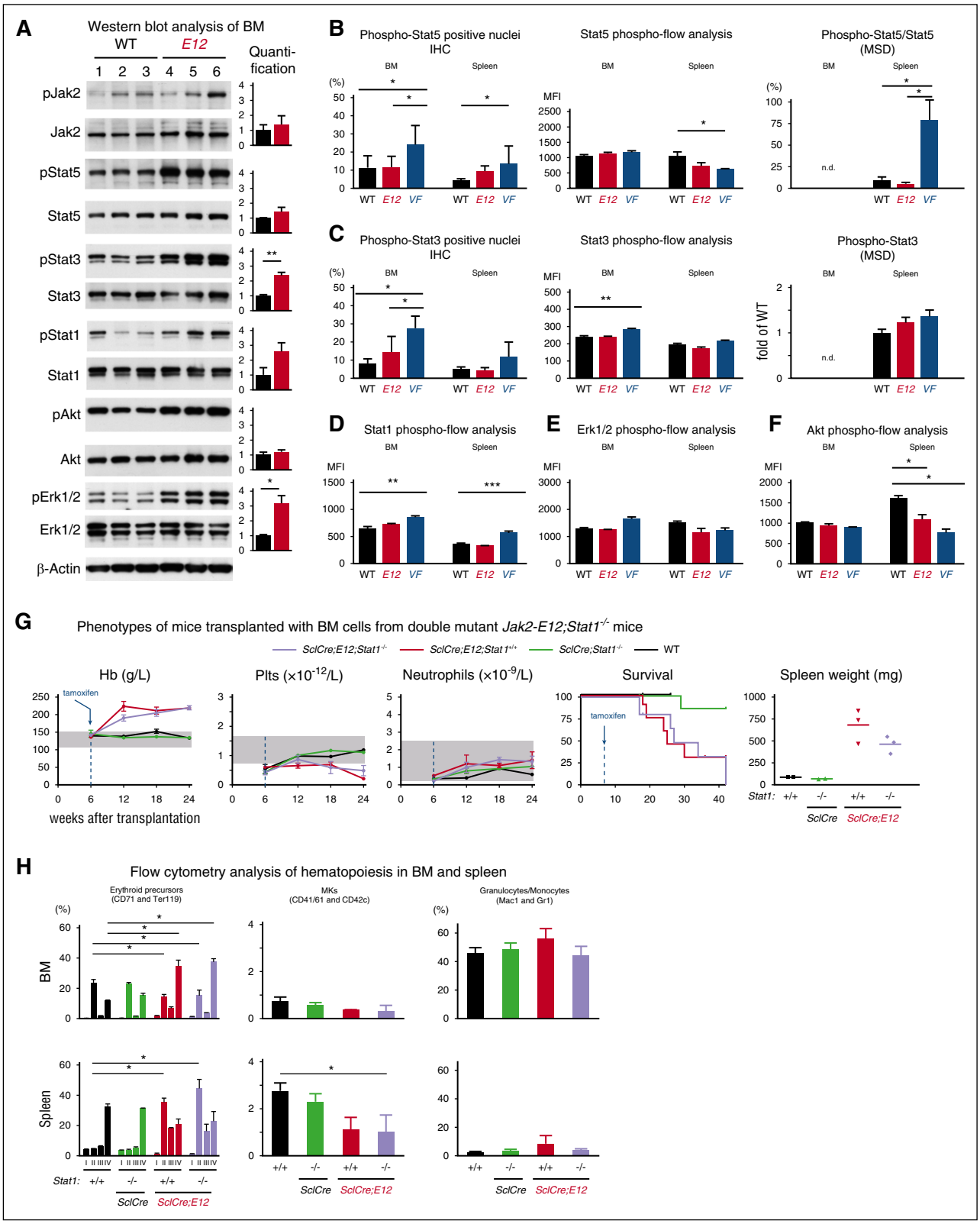

Figure 6. Analysis of Jak-Stat signaling in BM and spleen of *JAK2-Ex12* transgenic mice. (A) Western blot analysis of indicated total and phospho proteins in BM lysates from WT and *MxCre;Ex12* mice. Bar graphs represent the average ratio of phospho and total proteins for signal intensity of respective proteins (n = 3 per each genotype). (B) Phosphorylation levels of Stat5 protein at Tyr705 detected in nuclei of BM cells (sternum) and spleen cells by immunohistochemistry (IHC) staining. The histograms show the percentages of nuclei positive for phospho-Stat5 counted using the Aperio ImageScope image analysis software (left). The group sizes were: n = 10 for WT and *MxCre;Ex12* mice, and n = 6 for *MxCre;V617F* mice. The values represent the mean ± standard deviation. Intracellular phospho-flow analysis of phospho-Stat5 levels in BM and spleen from indicated mice (middle) (n = 6 per genotype). Relative levels of phospho-Stat5 protein measured in spleen cell lysates using the MSD (right). (C) Phosphorylation levels of Stat3 protein at Tyr705 detected in nuclei of BM cells (sternum) and spleen cells by immunohistochemistry staining. The histograms show the percentages of nuclei positive for phospho-Stat3 (left). The group sizes were: n = 10 for WT and *MxCre;Ex12* mice, and n = 6 for *MxCre;V617F* mice. Intracellular phospho-flow analysis of phospho-Stat3 levels in BM and spleen from

Downloaded from http://ashpublications.net/blood/article-pdf/128/6/839/1398408/839.pdf by guest on 18 May 2024

alterations suggest that iron metabolism is altered by the presence of the *JAK2 exon 12* mutations to optimize the availability of iron required for increased erythropoiesis.

Discussion

The hematologic phenotype of our *JAK2;Ex12* mutant mice with prominent erythrocytosis but normal platelets and neutrophils, closely resembles the phenotype observed in the majority of patients with a mutation in *JAK2 exon 12*.[20] The mean hemoglobin levels in our *JAK2;Ex12* mice were higher than hemoglobin levels in mice expressing *JAK2-V617F*. Similarly, PV patients with *JAK2 exon 12* mutations display higher hemoglobin values than PV patients carrying *JAK2-V617F*.[9] Nevertheless, in addition to erythrocytosis, about one-third of patients with *JAK2 exon 12* mutations also show thrombocytosis or leukocytosis, or a tri-lineage pattern.[9] The basis for these phenotypic differences is currently unknown. Co-occurrence of additional mutations in *TET2* has been described in patients with *JAK2 exon 12* mutations.[21,22] However, no systematic screening for additional mutations has been performed in larger cohorts of patients with *JAK2 exon 12* mutations, and therefore the frequency of additional somatic mutations remains unknown.

Our *JAK2;Ex12* mice showed no signs of myelofibrosis and no significant increase in megakaryopoiesis (Figure 4). Because the manifestation of myelofibrosis correlates with thrombocytosis and/or dysmegakaryopoiesis and the release of transforming growth factor-β and other mediators of fibrosis from platelets and megakaryocytes,[23-25] the absence of myelofibrosis in *JAK2;Ex12* mice fits well with the observed normal platelet counts. Analysis of progenitor populations revealed an increase in erythroid precursors, whereas megakaryopoiesis was not significantly altered (Figure 5). Myelofibrosis is rare in patients with *JAK2 exon 12* mutations, but nevertheless some cases have been described.[6,9,26] It remains to be determined whether this variability reflects species differences in Jak2 exon 12 signaling, or whether additional somatic gene mutations are responsible for thrombocytosis and myelofibrosis in some PV patients with *JAK2 exon 12* mutations.

Survival was reduced in *JAK2;Ex12* mice compared with both WT controls and *JAK2-V617F* mice (Figure 3B). Activation of the *Ex12* transgene by $SclCre^{ER}$ resulted in a shorter survival and a more pronounced erythropoietic phenotype than activation by *MxCre* (Figure 3; supplemental Figure 2). In agreement with our previous observations in $SclCre^{ER}$*;V617F* mice,[14] survival was improved when BM cells from $SclCre^{ER}$*;Ex12* or *MxCre;Ex12* mice was transplanted into lethally irradiated hosts (supplemental Figure 3), indicating that a nonhematopoietic component contributes to the lethality in nontransplanted mice. In most cases, the cause of death was difficult to establish, because the mice were found dead without previous signs of sickness, but in 2/9 $SclCre^{ER}$*;Ex12* mice we found intraperitoneal bleeding upon autopsy. A bleeding tendency was also documented by the presence of a hemoccult positive stool in 5/5 $SclCre^{ER}$*;Ex12* mice analyzed (supplemental Figure 3).

Although the Jak2 exon 12 mutations and Jak2-V617F activate the same C-terminal kinase domain of Jak2, the phenotypic readout of these Jak2 mutants in transgenic mice and patients is different. *JAK2-V617F* mutation can cause essential thrombocythemia (ET), PV, or primary myelofibrosis (PMF) phenotypes. Several factors can influence genotype-phenotype decisions in *JAK2-V617F* positive MPN, including the presence of subclones homozygous for *JAK2-V617F* favoring PV,[8,27,28] and activity of the IFN-γ/Stat1 signaling favoring ET.[18,19] Transgenic and knockin mice expressing *JAK2-V617F* also displayed phenotypes ranging from ET to PV and PMF.[29,30] The ratio between the expression of *JAK2-V617F* vs WT *Jak2* was shown to be one of the factors that can influence the choice between ET and PV, with higher expression levels of *JAK2-V617F* favoring PV.[12] Our *JAK2;Ex12* mice displayed erythrocytosis with very high hemoglobin values despite the fact that the ratio of *JAK2;Ex12* to WT *Jak2* mRNA expression was very low (Figure 2D). These data indicate that expression levels are not the basis for the phenotypic differences and suggest that there is a qualitative difference in the signals produced by the mutant *JAK2;Ex12* compared with *JAK2-V617F* on the phenotypic manifestation.

The presence of Jak2;Ex12 was associated with significantly increased baseline levels of pStat3 and pErk1/2, and a trend toward increased pStat5 and pStat1 compared with WT controls (Figure 6A). Because *Ex12* mice have normal or subnormal platelet counts, and Stat1 activity favors megakaryopoiesis and thrombocytosis, one might expect that Stat1 signaling would be decreased in *Ex12* mice.[18,19] Our data are in line with the recent results showing increased Stat1 activity in PV patients with *JAK2 exon 12* mutations, similar to ET patients with *JAK2*-V617F.[11] To clarify the role of Stat1 in Jak2-Ex12 signaling, we analyzed *Ex12;Stat1*$^{-/-}$ double-mutant mice and found that loss of Stat1 had no effects on blood counts or the composition of BM and spleen progenitor cells (Figure 6G-H), indicating that Stat1 does not play a central role in mediating the effects of Ex12 signaling on megakaryopoiesis or erythropoiesis. Finally, phosphorylation of Stat5 was not significantly increased compared with WT controls (Figure 6B), whereas Jak2-V617F significantly increased both pStat3 and pStat5 (Figure 6B-C). The lack of a significant increase of pStat5 in *JAK2;Ex12* mice is unexpected, because pStat5 is important for the pathogenesis of the MPN phenotype in JAK2-V617F mice.[31,32]

Tfr1 mRNA and protein expression was increased in *JAK2;Ex12* mice (Figure 7A-B). We therefore analyzed the expression of other key components of iron metabolism.[33,34] Although iron in the serum and liver showed no major changes (Figure 7C-D), we found that *Erfe* and *hepcidin* (*Hamp*) expression was inversely altered (Figure 7E-F). Erfe is a new hormone that is produced by erythroblasts and was shown to suppress hepcidin during stress erythropoiesis.[35,36] Hepcidin suppression does not require binding of Epo to Epo receptors in the liver, and recent data rather suggest that the role of Epo is to stimulate the synthesis of the erythroid regulator *ERFE* in erythroblasts, which ultimately downregulates *hepcidin*.[37] High Erfe and low hepcidin together with elevated Tfr1 result in a state that enhances iron resorption in the gut and assures efficient iron delivery to the sites of hematopoiesis, thereby favoring hyperactive erythropoiesis.[34] These changes in iron metabolism were more pronounced in *JAK2;Ex12*

Figure 6 (continued) indicated mice (middle). Relative levels of phospho-Stat3 protein measured in spleen cell lysates using the MSD technology (right). The values represent mean ± SEM (n = 3 per group). Intracellular phospho-flow analysis of (D) phospho-Stat1, (E) phospho-Erk1/2, and (F) phospho-Akt1 levels in BM and spleen from indicated mice. Values on Y-axis indicate the MFI of indicated proteins (n = 6 mice per genotype). One-way ANOVA with subsequent Bonferroni post-test was used. $^{*}P < .05$; $^{**}P < .01$; $^{***}P < .001$. (G) Blood counts, survival, and spleen weight of lethally irradiated recipient mice (n = 4 per group) transplanted with 1×10^6 BM cells from non-induced donor mice with the indicated genotypes. Tamoxifen was injected 6 weeks after transplantation, as indicated by the blue arrows. (H) Analysis of BM (top) and spleen (bottom) cells of transplanted mice euthanized 24 weeks after transplantation. MFI, mean fluorescence intensity.

Downloaded from http://ashpublications.net/blood/article-pdf/128/6/839/1398408/839.pdf by guest on 18 May 2024

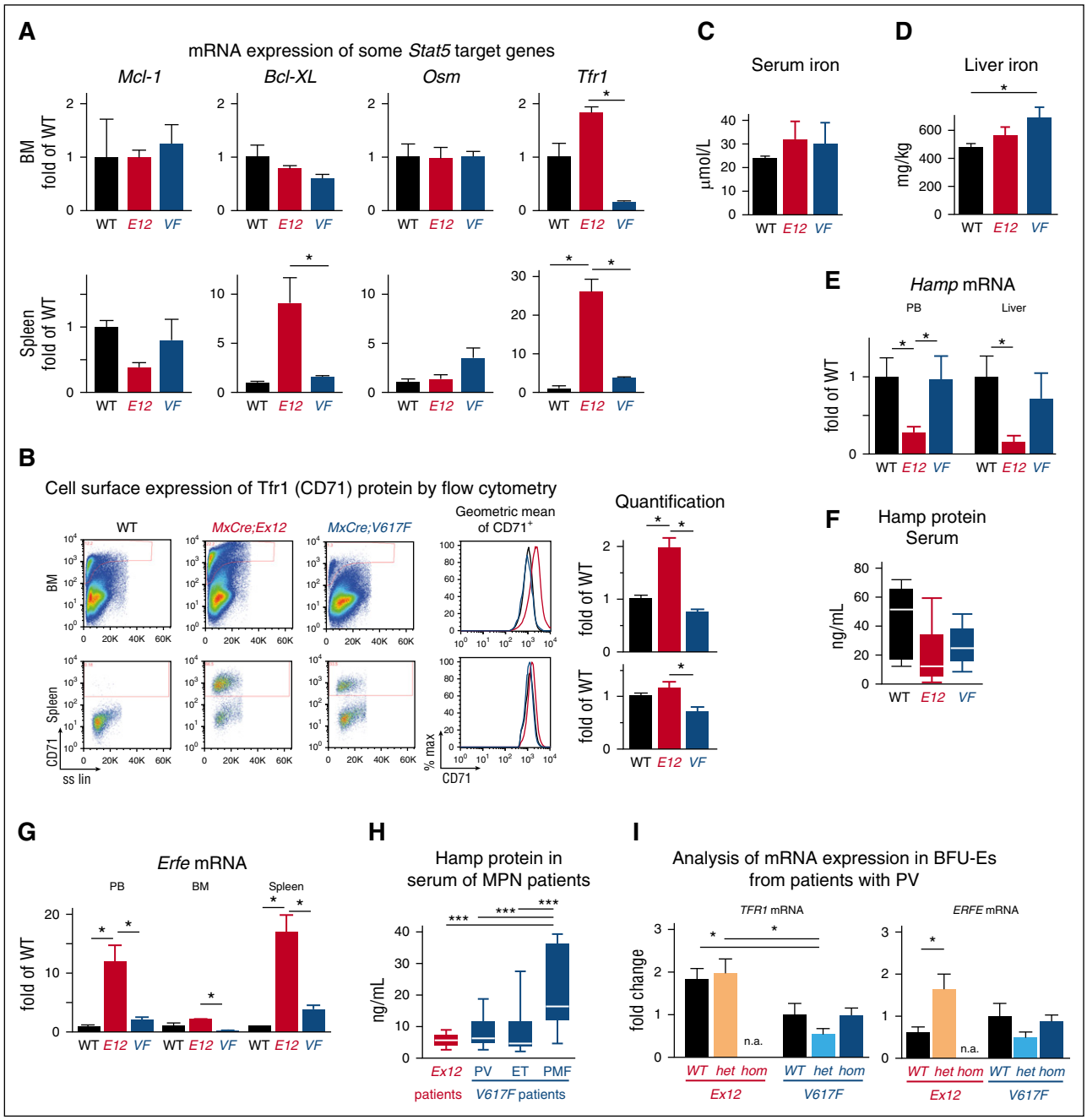

Figure 7. Altered expression of erythropoietic and iron metabolism regulators in *JAK2-Ex12* transgenic mice and erythroid precursors from PV patients with *JAK2-Ex12* mutation. (A) Expression of mRNA for *Mcl-1*, *Bcl-XL*, *Osm*, and *Tfr1* were determined by RT-PCR in *MxCre;Ex12* mice, *MxCre;V617F* mice, or WT controls (n = 3 per group). One-way ANOVA with subsequent Bonferroni post-test was used. **P* < .05. Mice were euthanized 12 weeks after *pIpC* injection. (B) Cell surface expression of Tfr1 (CD71) protein determined by flow cytometry. Representative flow cytometry plots of 1 mouse for each of the 3 genotypes (left). The geometric means of fluorescent intensities for CD71 are shown for the 3 genotypes (red, *Ex12*; blue, *V617F*; and black, WT) (middle). The quantification of the Tfr1 (CD71) cell surface expression from groups of 3 mice per genotype (right). Data are from 2 independent experiments. The mean of the CD71 fluorescent intensities ± SEM are shown as fold changes of the value found in WT mice. *E12*, *MxCre;Ex12* and *VF*, *MxCre;V617F*. (C) Serum iron levels. (D) Liver iron levels (n = 6 mice per genotype). (E) Expression of mRNA for *hepcidin* (*Hamp*) determined by RT-PCR (n = 3 per group). (F) Hepcidin protein concentration (ng/mL) in the serum measured by ELISA (n = 3 per group). (G) Expression of mRNA for *Erfe* were determined by RT-PCR (n = 3 per group). (H) Hepcidin protein concentration in the serum of PV patients with *JAK2 exon 12* mutations (n = 6) and in MPN patients with the *JAK2-V617F* mutation (PV, n = 10; ET, n = 12; and PMF, n = 10 patients per group). (I) Analysis of mRNA expression in BFU-E colonies from patients with PV. Peripheral blood mononuclear cells from 3 patients with *JAK2 exon 12* mutations and 2 patients with *JAK2*-V617F were grown in methylcellulose, and single BFU-E colonies were picked and genotyped for *JAK2 exon 12* mutations (red) or *JAK2-V617F* (blue), respectively. The mRNA from each colony was individually analyzed for *TFR1* and *ERFE* expression by RT-PCR and the mean ± SEM values for all *JAK2* (WT), heterozygous (het), and homozygous (hom) *JAK2* mutant colonies are shown as the fold changes of the values obtained in WT colonies from the *JAK2-V617F* positive patients. The patients with *JAK2 exon 12* mutations were only heterozygous, and homozygous colonies were not available. One-way ANOVA with subsequent Bonferroni post-test was used. **P* < .05; ****P* < .001. n.a., not available.

mice than in our *JAK2-V617F* mice, and may contribute to the more prominent erythrocytosis observed in *JAK2;Ex12* mice compared with *JAK2-V617F* mice. In line with a previous report,[38] serum hepcidin levels were significantly elevated in PMF patients with JAK2-V617F (Figure 7H). Consistently, a trend toward increased *TFR1* and *ERFE* mRNA expression was also noted in BFU-E

Downloaded from http://ashpublications.net/blood/article-pdf/128/6/839/1398408/839.pdf by guest on 18 May 2024

colonies from PV patients with *JAK2* exon 12 mutation compared with PV patients with *JAK2*-V617F (Figure 7I).

Our mice expressing the most prevalent *JAK2 exon 12* mutation (*N542-E543del* mutation) faithfully reproduce the isolated PV-like phenotype observed in the majority of PV patients with JAK2 exon 12 mutations. These data suggest that there are qualitative differences in the signals produced by the mutant JAK2;Ex12 protein, in particular with respect to collaborating with Stat1 signaling. A prominent consequence of altered signaling by *JAK2-N542-E543del* are changes in the expression levels of key regulators of iron metabolism that increase iron availability to allow maximal production of red cells.

Acknowledgments

The authors thank Toni Krebs and Emmanuel Traunecker (Flow Facility, Department of Biomedicine, University Hospital Basel) for their valuable technical assistance with cell sorting and flow cytometry analysis, and David E. Levy for providing the *Stat1* knockout mice. The authors also thank Adrian Duek, Takafumi Shimizu, Jakub Zmajkovic, Morgane Hilpert, Ronny Nienhold, and Ralph Tiedt for helpful discussions.

This work was supported by grants from the Swiss National Science Foundation (310000-120724/1 and 32003BB_135712/1) and the Swiss Cancer League (KLS-2950-02-2012 and KFS-3655-02-2015) (R.C.S.).

Authorship

Contribution: J.G., S.L., and T.N.R. designed research, performed research, analyzed data, and wrote the paper; L.K., S.C.M., P.L., H.H.-S., V.R., M.M., and T.R. performed research and analyzed data; S.D. prepared and analyzed histology samples; and R.C.S. designed research, analyzed data, and wrote the paper.

Conflict-of-interest disclosure: V.R., M.M., and T.R. are full-time employees of Novartis Pharma AG. The remaining authors declare no competing financial interests.

Correspondence: Radek C. Skoda, Department of Biomedicine, Experimental Hematology, University Hospital Basel, Hebelstr 20, 4031 Basel, Switzerland; e-mail: radek.skoda@unibas.ch.

References

1. James C, Ugo V, Le Couédic JP, et al. A unique clonal JAK2 mutation leading to constitutive signalling causes polycythaemia vera. *Nature.* 2005;434(7037):1144-1148.
2. Baxter EJ, Scott LM, Campbell PJ, et al; Cancer Genome Project. Acquired mutation of the tyrosine kinase JAK2 in human myeloproliferative disorders. *Lancet.* 2005; 365(9464):1054-1061.
3. Levine RL, Wadleigh M, Cools J, et al. Activating mutation in the tyrosine kinase JAK2 in polycythemia vera, essential thrombocythemia, and myeloid metaplasia with myelofibrosis. *Cancer Cell.* 2005;7(4):387-397.
4. Kralovics R, Passamonti F, Buser AS, et al. A gain-of-function mutation of JAK2 in myeloproliferative disorders. *N Engl J Med.* 2005; 352(17):1779-1790.
5. Scott LM, Tong W, Levine RL, et al. JAK2 exon 12 mutations in polycythemia vera and idiopathic erythrocytosis. *N Engl J Med.* 2007;356(5): 459-468.
6. Pardanani A, Lasho TL, Finke C, Hanson CA, Tefferi A. Prevalence and clinicopathologic correlates of JAK2 exon 12 mutations in JAK2V617F-negative polycythemia vera. *Leukemia.* 2007;21(9):1960-1963.
7. Pietra D, Li S, Brisci A, et al. Somatic mutations of JAK2 exon 12 in patients with JAK2 (V617F)-negative myeloproliferative disorders. *Blood.* 2008;111(3):1686-1689.
8. Li S, Kralovics R, De Libero G, Theocharides A, Gisslinger H, Skoda RC. Clonal heterogeneity in polycythemia vera patients with JAK2 exon12 and JAK2-V617F mutations. *Blood.* 2008;111(7): 3863-3866.
9. Passamonti F, Elena C, Schnittger S, et al. Molecular and clinical features of the myeloproliferative neoplasm associated with JAK2 exon 12 mutations. *Blood.* 2011;117(10): 2813-2816.
10. Vardiman JW, Thiele J, Arber DA, et al. The 2008 revision of the World Health Organization (WHO) classification of myeloid neoplasms and acute leukemia: rationale and important changes. *Blood.* 2009;114(5):937-951.
11. Godfrey AL, Chen E, Massie CE, et al. STAT1 activation in association with JAK2 exon 12 mutations. *Haematologica.* 2016;101(1): e15-e19.
12. Tiedt R, Hao-Shen H, Sobas MA, et al. Ratio of mutant JAK2-V617F to wild-type Jak2 determines the MPD phenotypes in transgenic mice. *Blood.* 2008;111(8):3931-3940.
13. Kühn R, Schwenk F, Aguet M, Rajewsky K. Inducible gene targeting in mice. *Science.* 1995; 269(5229):1427-1429.
14. Kubovcakova L, Lundberg P, Grisouard J, et al. Differential effects of hydroxyurea and INC424 on mutant allele burden and myeloproliferative phenotype in a JAK2-V617F polycythemia vera mouse model. *Blood.* 2013; 121(7):1188-1199.
15. Durbin JE, Hackenmiller R, Simon MC, Levy DE. Targeted disruption of the mouse Stat1 gene results in compromised innate immunity to viral disease. *Cell.* 1996;84(3): 443-450.
16. Zhang Z, Lutz B. Cre recombinase-mediated inversion using lox66 and lox71: method to introduce conditional point mutations into the CREB-binding protein. *Nucleic Acids Res.* 2002; 30(17):e90.
17. Lundberg P, Takizawa H, Kubovcakova L, et al. Myeloproliferative neoplasms can be initiated from a single hematopoietic stem cell expressing JAK2-V617F. *J Exp Med.* 2014;211(11): 2213-2230.
18. Chen E, Beer PA, Godfrey AL, et al. Distinct clinical phenotypes associated with JAK2V617F reflect differential STAT1 signaling. *Cancer Cell.* 2010;18(5):524-535.
19. Duek A, Lundberg P, Shimizu T, et al. Loss of Stat1 decreases megakaryopoiesis and favors erythropoiesis in a JAK2-V617F-driven mouse model of MPNs. *Blood.* 2014;123(25): 3943-3950.
20. Scott LM. The JAK2 exon 12 mutations: a comprehensive review. *Am J Hematol.* 2011; 86(8):668-676.
21. Schaub FX, Looser R, Li S, et al. Clonal analysis of TET2 and JAK2 mutations suggests that TET2 can be a late event in the progression of myeloproliferative neoplasms. *Blood.* 2010; 115(10):2003-2007.
22. Lundberg P, Karow A, Nienhold R, et al. Clonal evolution and clinical correlates of somatic mutations in myeloproliferative neoplasms. *Blood.* 2014;123(14):2220-2228.
23. Villeval JL, Cohen-Solal K, Tulliez M, et al. High thrombopoietin production by hematopoietic cells induces a fatal myeloproliferative syndrome in mice. *Blood.* 1997;90(11):4369-4383.
24. Gastinne T, Vigant F, Lavenu-Bombled C, et al. Adenoviral-mediated TGF-beta1 inhibition in a mouse model of myelofibrosis inhibit bone marrow fibrosis development. *Exp Hematol.* 2007;35(1): 64-74.
25. Chagraoui H, Komura E, Tulliez M, Giraudier S, Vainchenker W, Wendling F. Prominent role of TGF-beta 1 in thrombopoietin-induced myelofibrosis in mice. *Blood.* 2002;100(10): 3495-3503.
26. Butcher CM, Hahn U, To LB, et al. Two novel JAK2 exon 12 mutations in JAK2V617F-negative polycythaemia vera patients. *Leukemia.* 2008; 22(4):870-873.
27. Scott LM, Scott MA, Campbell PJ, Green AR. Progenitors homozygous for the V617F mutation occur in most patients with polycythemia vera, but not essential thrombocythemia. *Blood.* 2006; 108(7):2435-2437.
28. Godfrey AL, Chen E, Pagano F, et al. JAK2V617F homozygosity arises commonly and recurrently in PV and ET, but PV is characterized by expansion of a dominant homozygous subclone. *Blood.* 2012;120(13):2704-2707.
29. Li J, Kent DG, Chen E, Green AR. Mouse models of myeloproliferative neoplasms: JAK of all grades. *Dis Model Mech.* 2011;4(3): 311-317.
30. Van Etten RA, Koschmieder S, Delhommeau F, et al. The Ph-positive and Ph-negative myeloproliferative neoplasms: some topical pre-clinical and clinical issues. *Haematologica.* 2011; 96(4):590-601.

Downloaded from http://ashpublications.net/blood/article-pdf/128/6/839/1398408/839.pdf by guest on 18 May 2024

31. Yan D, Hutchison RE, Mohi G. Critical requirement for Stat5 in a mouse model of polycythemia vera. *Blood.* 2012;119(15): 3539-3549.

32. Walz C, Ahmed W, Lazarides K, et al. Essential role for Stat5a/b in myeloproliferative neoplasms induced by BCR-ABL1 and JAK2(V617F) in mice. *Blood.* 2012;119(15): 3550-3560.

33. Camaschella C. Iron-deficiency anemia. *N Engl J Med.* 2015;373(5):485-486.

34. Ganz T, Nemeth E. Iron homeostasis in host defence and inflammation. *Nat Rev Immunol.* 2015;15(8):500-510.

35. Kautz L, Jung G, Valore EV, Rivella S, Nemeth E, Ganz T. Identification of erythroferrone as an erythroid regulator of iron metabolism. *Nat Genet.* 2014;46(7):678-684.

36. Kautz L, Jung G, Du X, et al. Erythroferrone contributes to hepcidin suppression and iron overload in a mouse model of β-thalassemia. *Blood.* 2015;126(17):2031-2037.

37. Gammella E, Diaz V, Recalcati S, et al. Erythropoietin's inhibiting impact on hepcidin expression occurs indirectly. *Am J Physiol Regul Integr Comp Physiol.* 2015;308(4): R330-R335.

38. Pardanani A, Finke C, Abdelrahman RA, Lasho TL, Tefferi A. Associations and prognostic interactions between circulating levels of hepcidin, ferritin and inflammatory cytokines in primary myelofibrosis. *Am J Hematol.* 2013;88(4): 312-316.

Downloaded from http://ashpublications.net/blood/article-pdf/128/6/839/1398408/839.pdf by guest on 18 May 2024